Solid-on-solid models of molecular-beam epitaxy

Martin Siegert
Theoretische Physik, FB 10, Universität Duisburg, 47048 Duisburg, Germany

Michael Plischke
Physics Department, Simon Fraser University, Burnaby, British Columbia, Canada V5A 1S6
(Received 21 December 1993)

We discuss a number of solid-on-solid models that contain the two most important features of molecular-beam epitaxy: a flux of particles and relaxation of the growing film by surface diffusion. Evaporation of particles is not allowed and surface diffusion is driven by a Hamiltonian containing short-range interactions. In the absence of deposition, the correct equilibrium phase is recovered. We find that there are two generic situations depending on whether or not diffusing particles are repelled from step edges by so-called Schwoebel barriers: (i) Positive Schwoebel barriers lead to unstable growth and the formation of pyramidlike structures. (ii) Negative Schwoebel barriers result in surface roughness that scales only logarithmically with separation or system size. This class is described at large length scales by the Edwards-Wilkinson equation. The atypical case of no Schwoebel barrier occurs only if there is a special symmetry in the diffusion process. This scenario is present regardless of whether surface diffusion is implemented through an Arrhenius process or through Metropolis-type hopping rates. We conclude that, at least in the context of solid-on-solid models, there are only two generic universality classes. These results are discussed in terms of a general Langevin equation and related to recent experiments.

PACS number(s): 05.40.+j, 61.50.Cj, 05.70.Ln, 68.55.Bd

I. INTRODUCTION

During the past decade, it has become evident that many nonequilibrium growth processes display power-law behavior in space and time similar to that found at the critical point of systems undergoing continuous phase transitions. To be precise, if the surface of a growing cluster can be described in terms of a variable $h(\mathbf{r},t)$, it is generically found that the correlation function

$$G(\mathbf{r},t) \equiv \langle [h(\mathbf{r},t) - h(0,t)]^2 \rangle = r^{2\zeta} g(r/\xi(t)) \ , \qquad (1.1)$$

where $\xi(t) \sim t^{1/z}$. The two exponents ζ and z, along with the asymptotic form of the scaling function g—discussed in more detail below—characterize the growth process in question. It is therefore of great interest to examine to what extent this type of scaling holds and to what extent the concept of universality, familiar from equilibrium phase transitions, is relevant for nonequilibrium growth processes. Considerable progress has been made in this endeavor. For example, growth processes such as the Eden process [1], ballistic deposition [2], and growth of various restricted solid-on-solid models [3] are well described by the Kardar-Parisi-Zhang (KPZ) [4] equation, a nonlinear Langevin equation for which one can show rigorously (at least in one dimension) that the aforementioned power-law behavior obtains. The processes listed above have the property that the velocity of the growing cluster is in a direction locally perpendicular to the existing surface and this is sufficient to ensure the presence of the KPZ nonlinearity as well as the linear Edwards-Wilkinson term [5] in the continuum representation of these models.

A quite different situation exists in molecular-beam epitaxy (MBE), where particles are deposited through a directed beam rather than through vapor deposition. Usually, evaporation is negligible during MBE growth and the surface of the sample relaxes entirely through surface diffusion. In addition, in most cases, voids and overhangs can be neglected, at least on time scales long compared to atomic time scales. Therefore, it is reasonable to model MBE growth by solid-on-solid (SOS) models. These two considerations (no evaporation and no overhangs) give rise to a conservation law that forbids the KPZ nonlinearity in the continuum limit:

$$\partial_t h(\mathbf{r},t) + \nabla \cdot \mathbf{j}(\mathbf{r},t) = F + \eta(\mathbf{r},t) \ . \qquad (1.2)$$

Here $\mathbf{j}(\mathbf{r},t)$ is the surface diffusion current and F and $\eta(\mathbf{r},t)$ represent the beam intensity and its fluctuations. Therefore, these models, as well as MBE, are expected to be in a universality class different from that of the KPZ equation.

Early attempts to implement these criteria in discrete models of MBE were made by Wolf and Villain [6] and Das Sarma and Tamborenea [7]. These authors, in the interest of computational efficiency, combined random deposition with a very simple realization of the surface diffusion process: a newly deposited particle is allowed one move to a nearest-neighbor site if this move results in a higher coordination number. These models produced unreasonably large values of ζ and, moreover [8], have been shown to have a more complicated scaling form than that of (1.1).

More recently, we and others [9–12] have attempted to model MBE in a way that allows the surface to relax in a more realistic way. In particular, all particles that are not fully coordinated are allowed to diffuse by nearest-neighbor hopping between deposition events. Detailed balance is required for the diffusion process and this ensures that the appropriate equilibrium phase (flat or rough) is recovered when the deposition rate is set to zero. Surprisingly, when Metropolis dynamics [13] is used for the hopping rates, the kinetic universality class of this type of model depends sensitively on the details of the energy function that drives the diffusion process. Two types of behavior are generic: (i) for one class of models conventional scaling with Edwards-Wilkinson exponents is found; (ii) a second class of models [completely equivalent to class (i) in the equilibrium case] is unstable towards the formation of large slopes and pyramidal structures. An intermediate nontypical case displays conventional scaling with classical exponents [$z = 4, \zeta = (z-d)/2$]. This dependence on the details of the surface Hamiltonian can be traced back to the existence of Schwoebel barriers [14] for a certain parameter range. On the other hand, when diffusion is modeled by an Arrhenius process [15–17] classes (i) and (ii) appear generically if Schwoebel barriers are implemented in the diffusion rates as well. In the absence of Schwoebel barriers, corresponding to the nontypical case of Metropolis dynamics, the exponents ζ and z are consistent with the predictions of the conserved KPZ equation [18].

In this article we report primarily our results for a number of one- and two-dimensional models with diffusion governed by Metropolis dynamics. In Sec. II we introduce the various models and discuss in more detail the scaling of the correlation functions and how these functions relate to experiment. In Sec. III we turn to the representation of models of MBE by Langevin equations. Section IV contains the bulk of our numerical results for Metropolis dynamics. In Sec. V we present results for Arrhenius dynamics with and without Schwoebel barriers and relate them to those of Sec. IV. Finally, we present a short discussion and an outlook for the future in Sec. VI.

II. MODEL

As noted above, two processes are most important for a theoretical description of MBE: particle deposition and surface diffusion. The simplest possible model for surface diffusion is to assume that it is controlled by the same Hamiltonian $\mathcal{H}$ that controls the roughening of a facet in the absence of deposition. It is then a simple matter to add random deposition to this process and this is our basic microscopic model. In a computer simulation of such a model, a lattice site i is randomly selected and a particle is deposited at that site with probability $f < 1$. A diffusive move is attempted with probability $1-f$. In the latter case a nearest-neighbor site j is chosen at random and the move is accepted with a hopping probability $w_{i\to j}$. To implement the Metropolis dynamics mentioned in the Introduction, we have chosen the normalized hopping rates

$$w_{i\to j} = \left[1+\exp\left(\frac{1}{k_BT}\Delta\mathcal{H}_{i\to j}\right)\right]^{-1} = \frac{1}{2}\left[1-\tanh\left(\frac{1}{2k_BT}\Delta\mathcal{H}_{i\to j}\right)\right] . \tag{2.1}$$

Here $\Delta\mathcal{H}_{i\to j}$ is the energy difference between the final and initial states of the move. The hopping rates (2.1) preserve detailed balance in the absence of deposition and thus ensure that in such a case, the proper equilibrium state is reached. The surface energy we use in our Monte Carlo simulations is defined through the Hamiltonian of an *unrestricted* SOS model,

$$\mathcal{H} = \frac{1}{2}J\sum_{\langle i,j\rangle}|h_i-h_j|^n , \tag{2.2}$$

where $\langle i,j\rangle$ denotes the summation over nearest neighbors on a d-dimensional lattice, $d = 1,2$ is the substrate dimension, h_i is the (integer) height variable at site i, and n is a positive number that, in our simulations, we have taken to be $n = 1$, 2, or 4, although in general n need not be an integer.

The significance of n is the following: Consider a vicinal surface of large terraces separated by single steps. A diffusing particle obeying the dynamics of the $n = 1$ model performs a random walk on such a surface until it reaches a step where it becomes incorporated into the substrate (at least at low temperatures we can neglect the emission of particles from step edges). When a particle approaches a step from the upper terrace it has to create a double step at the step edge. In the $n = 1$ model the energy of a double step is the same as the energy of two single steps. Therefore, this intermediate state does not cost extra energy in the $n = 1$ model. This is no longer true for $n > 1$: In these cases a diffusing particle is repelled from a down step and will preferably diffuse in the uphill direction. Such an uphill current constitutes the "Schwoebel effect" and the potential barriers responsible for the effect are commonly called "Schwoebel barriers" [14] and have been discussed in detail by Villain [18]. The size of these barriers depends on material properties, e.g., the lattice structure or the orientation of the surface. The above argument naively implies that there is no Schwoebel effect in the $n = 1$ model. However, we will show in Sec. IV that this is not correct because this argument considers only configurations with widely separated steps. In Sec. IV we will show that there is no Schwoebel effect in the $n = 2$ model, a negative Schwoebel effect in the $n = 1$ model leading to current of diffusing particles in the downhill direction, and a positive Schwoebel effect for $n > 2$. Nevertheless, the above argument qualitatively explains the increase of the Schwoebel barriers with increasing n.

The ratio $(1-f)/f$ corresponds to the ratio of the diffusion constant D of particles on a flat surface to the incoming particle flux F. The quantity D/F plays an important role in determining the surface morphology at early times when layer-by-layer growth can be observed [19]. If isotropic diffusion on the terraces is assumed and dimers are regarded as stable clusters, it is found that

the average distance l_d between nucleation sites increases as $l_d \sim (D/F)^{1/6}$ [20,19]. Experimentally l_d is of the order of $10 - 100$ corresponding to $D/F = 10^6 - 10^{12}$ [21,22], depending on the temperature of the substrate. In numerical simulations usually much smaller values are used in order to observe the effects of kinetic surface roughening within reasonable computer time. For this reason the early time behavior is generally not observed, although these simple models are capable of describing this regime. Figure 1 shows oscillations of the density $d(t) = (N_{\text{even}} - N_{\text{odd}})/N$ over the time of 20 deposited monolayers for $f = 10^{-5}$ and $n = 1$. N_{even} (N_{odd}) denotes the number of sites with h_i even (odd) and $N = N_{\text{even}} + N_{\text{odd}} = L^2$. The function $d^2(t)$ is in many cases [23] proportional to the intensity of the specular spot in a reflection high-energy electron diffraction (RHEED) experiment during layer-by-layer growth if the angle of the electron beam is chosen so that electrons from neighboring layers interfere destructively. Since f is still relatively large by experimental standards the oscillations appear strongly damped. The disappearance of the RHEED oscillations coincides with the buildup of a stationary step density. This does not necessarily mean that the surface is rough [22]. In fact the difference between the maximum and the minimum of a typical height configuration at the latest time shown in Fig. 1 is about four layers. Kinetic roughening, as discussed below, sets in well after the RHEED oscillations have vanished.

The phenomenon of kinetic roughening is characterized by a correlation length ξ, which is also the typical wavelength of fluctuations on the growing surface. This correlation length grows as a power law $\xi(t) \sim t^{1/z}$. Associated with the increase of the correlation length ξ is the growing width of the surface $W(t) \sim [\xi(t)]^{\zeta}$. The dynamical exponent z and the roughness exponent ζ are believed to be universal, i.e., they depend on the growth conditions, but not on the microscopic details of the system. The power-law dependence of the correlation length signifies that the growth process occurs in a critical state and results in scale invariant surfaces. This, in turn, gives rise to scaling laws for

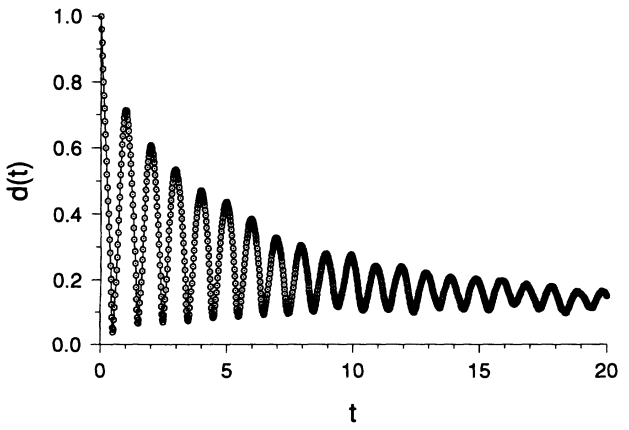

FIG. 1. Oscillations of the density $d(t)$ (see text) for $L^2 = 32 \times 32$, $k_B T/J = 0.1$, $f = 10^{-5}$, and $n = 1$.

the correlation functions. In the cases that are understood best the height-height correlation function (1.1) $G(\mathbf{r},t) \equiv L^{-d} \sum_{\mathbf{r}'} \langle [h(\mathbf{r}+\mathbf{r}',t) - h(\mathbf{r}',t)]^2 \rangle$ has the scaling form [24]

$$G(\mathbf{r},t) = r^{2\zeta} g(r/\xi(t)) \ . \tag{2.3}$$

The scaling function $g(x)$ is constant for $x \ll 1$ and compensates the r dependence for $x \gg 1$, i.e., $g(x) \sim x^{-2\zeta}$. These two limits can be used to calculate the exponents in a numerical simulation. However, using this function to determine ζ in the steady state, where the correlation length is equal to the system size, can be difficult, especially when crossover effects are important: Since the asymptotic behavior is dominated by the long wavelengths, one is interested in the large $r = |\mathbf{r}|$ behavior of $G(\mathbf{r},t)$. The large r regime of $G(\mathbf{r},t)$, however, is always distorted since the periodic boundary conditions, typically used in simulations, constrain $G(\mathbf{r},t)$ to have zero slope at $r = L/2$. This finite-size effect makes it necessary to determine ζ in a regime $1 \ll r \ll L/2$. The same problem does not exist if one concentrates on the structure factor

$$S(\mathbf{k},t) \equiv \langle \hat{h}(\mathbf{k},t) \hat{h}(-\mathbf{k},t) \rangle \tag{2.4}$$

with $\hat{h}(\mathbf{k},t) = L^{-d/2} \sum_{\mathbf{r}} [h(\mathbf{r},t) - \bar{h}] e^{i\mathbf{k}\mathbf{r}}$, where $\bar{h}$ is the spatial average of $h(\mathbf{r},t)$. The scaling form of this function is

$$S(\mathbf{k},t) = k^{-\gamma} s(k^z t) \tag{2.5}$$

with $\gamma = 2\zeta + d$. The scaling function s approaches a constant for large argument, but behaves differently in the short time limit $x \ll 1$ for $\gamma \leq z$, where $s(x) \sim x$, and $\gamma \geq z$, where $s(x) \sim x^{\gamma/z}$. If the growth process can be described through a Langevin equation of type (1.2) the hyperscaling relation [6]

$$\gamma = z \tag{2.6}$$

holds and we have $S(\mathbf{k},t) \sim t$ reflecting the fact that k modes with $k < 1/\xi(t)$ grow in an uncorrelated fashion. In the steady state the asymptotic behavior of the exponent γ is given through the small k behavior of $S(\mathbf{k}) \equiv S(\mathbf{k}, t \to \infty)$. The divergence of $S(\mathbf{k})$ for $k \to 0$ is not rounded by finite size effects, which affect only the behavior near $k = \pi$ [25]. Additionally, the computer time necessary to calculate $S(\mathbf{k},t)$ is of order $L^d \ln L$, whereas the time to calculate $G(\mathbf{r},t)$ increases as L^{2d}. The height-height correlation function G can be calculated using the Fourier transform of S,

$$G(\mathbf{r},t) = 2L^{-d} \sum_{\mathbf{k}} (1 - e^{-i\mathbf{k}\mathbf{r}}) S(\mathbf{k},t) \ . \tag{2.7}$$

To get an independent measure of the dynamical exponent z one can measure the time-time correlation function in the steady state [26,3,9,10]:

$$\Phi(\mathbf{k},t) \equiv \lim_{t' \to \infty} \langle \hat{h}(\mathbf{k}, t+t') \hat{h}(-\mathbf{k},t') \rangle / S(\mathbf{k}) \ . \tag{2.8}$$

Since Φ is a function of a single argument $\Phi(\mathbf{k},t) = \varphi(k^z t)$, the exponent z can be determined with quite high accuracy.

The width of the surface, $W^2(l,t) = l^{-d}\sum_{\mathbf{r}}\langle h^2(\mathbf{r},t)\rangle$ with $r_i \leq l$, has been measured by means of scanning tunneling microscopy and used to characterize the roughness of growing surfaces [27]. In numerical calculations l is usually set to the system size L and, if the scaling laws (2.5) and (2.3) hold, W scales as

$$W(l,t) = l^{\zeta} w(t/l^z) \tag{2.9}$$

with $w(x) \sim x^{\zeta/z}$ for $x \ll 1$ and $w(x) = \text{const}$ for $x \gg 1$. The width is easily calculated from either $S(\mathbf{k},t)$ or $G(\mathbf{r},t)$: $W^2(L,t) = L^{-d}\sum_{\mathbf{k}} S(\mathbf{q},t) = (1/2L^d)\sum_{\mathbf{r}} G(\mathbf{r},t)$. As W is the sum over these correlation functions, W contains less information about the system than the correlation functions themselves, e.g., W does not allow a check of the underlying scaling behavior (2.5) or (2.3) of the correlation functions. It has been shown [28,29] that models with $\gamma \geq d+2$ do not obey the scaling law (2.3). In such cases there is an ambiguity in the definition of ζ since (2.5) and (2.3) imply different values. But even for the physically relevant models with $\zeta < 1$ the standard scaling assumptions (2.5) and (2.3) can be violated [8,30] and this has led to incorrect assignments [31] of models to universality classes. Thus a determination of the exponents based solely on the calculation of $W(L,t)$ without a check of the underlying scaling laws (2.5) and (2.3) has to be treated with caution. We will show in Sec. IV that, in the case of unstable growth, results for $W(L,t)$ are misleading as well. We emphasize that, e.g., in scanning tunnel microscopy, $W(l,t)$ is measured as a function of l at fixed system size L. This measurement yields the same values for ζ as are obtained from $S(\mathbf{k},t)$ and $G(\mathbf{r},t)$ provided $\zeta < 1$.

We conclude this section by discussing the scaling functions that are accessible in experiments. As mentioned above, the width $W(l,t)$ and the height-height correlation function $G(\mathbf{r},t)$ are directly measurable in scanning tunnel microscopy experiments [27]. In atom diffraction, x-ray diffraction, and light scattering experiments one measures the diffraction structure factor [32,33]

$$\tilde{S}(\mathbf{k}_{\parallel},k_{\perp},t) = \int d^2r \exp\left[-\frac{k_{\perp}^2}{2}G(\mathbf{r},t)\right] e^{i\mathbf{k}_{\parallel}\cdot\mathbf{r}} \ . \tag{2.10}$$

If the condition $k_{\perp}W(t) \ll 1$ is fulfilled [$W(t) = \lim_{l\to\infty} W(l,t)$], as may be the case in light scattering experiments, one can expand the first exponential in (2.10) to linear order. In this case $\tilde{S}(\mathbf{k}_{\parallel},k_{\perp},t)$ as a function of $\mathbf{k}_{\parallel}$ and t is up to a prefactor $k_{\perp}^2$ and up to a δ-function contribution at $\mathbf{k}_{\parallel} = \mathbf{0}$ identical to $S(\mathbf{k},t)$ (2.4). The case $k_{\perp}W(t) \gg 1$ is discussed in [32].

III. LANGEVIN EQUATIONS

In this section we introduce the Langevin equation that potentially describes kinetic roughening phenomena in MBE. This approach goes back to the work of Mullins [34]. In the case of pure surface diffusion ($F = 0$) when the system relaxes to the equilibrium state and therefore detailed balance is obeyed, the normal velocity of the surface obeys a continuity equation

$$v_n(\mathbf{r},t) = -\nabla\cdot\left[\mathbf{j}(\mathbf{r},t) - \boldsymbol{\eta}_c(\mathbf{r},t)\right] \ . \tag{3.1}$$

Here $\boldsymbol{\eta}_c$ is a noise term describing the thermal fluctuations of the surface current $\langle\boldsymbol{\eta}_c(\mathbf{r},t)\rangle = 0$. The current density $\mathbf{j}$ is related to the surface chemical potential μ through Fick's law

$$\mathbf{j} = -\Lambda\nabla\mu \ . \tag{3.2}$$

The operator ∇ in (3.1,3.2) must be computed in a local coordinate system with the axes parallel to the surface. The kinetic coefficient may depend on the local tilt and the curvature tensor κ of the surface $\Lambda = \Lambda(\nabla h,\kappa)$. The chemical potential is obtained from the surface free energy $\mu = \delta\mathcal{F}/\delta h$. This relation reduces to the Herring equation [35] if $\mathcal{F}$ is taken to be the free energy functional of the drumhead model,

$$\mathcal{F} = \mathcal{F}_{\mathrm{DH}} = \int d^dx\, \sigma\sqrt{g} \quad \text{with} \quad g = 1 + (\nabla h)^2 \ . \tag{3.3}$$

The surface tension is, in general, anisotropic, $\sigma = \sigma(\nabla h)$. In principle, a pinning term $V\cos[2\pi h(\mathbf{r},t)]$ also has to be included in the integrand of (3.3). Such a term is crucial for a correct continuum description of the roughening transition of a two-dimensional surface [36]. Here we shall use (3.3) to derive the equation of motion for MBE, which describes moving surfaces. In this case, the pinning term is averaged to zero [36] and we therefore omit it in (3.3), although it should be included in the discussion of equilibrium relaxation. Due to this omission the equation of motion for the equilibrium surface below will result in a roughening temperature of zero.

Using the relation $v_n = \partial_t h/\sqrt{g}$ we arrive at the equation of motion for relaxation into the equilibrium state:

$$\partial_t h = \sqrt{g}\left(\Gamma_c\frac{\delta\mathcal{F}}{\delta h} + \nabla\cdot\boldsymbol{\eta}_c\right) \ . \tag{3.4}$$

The operator Γ_c is related to the intrinsic Laplace operator of the surface [37]

$$\Gamma_c = \frac{1}{\sqrt{g}}\frac{\partial}{\partial x_i}\left[\Lambda\sqrt{g}\left(\delta_{ij} - \frac{\partial h}{\partial x_i}\frac{\partial h}{\partial x_j}\right)\right]\frac{\partial}{\partial x_j} \ .$$

Equation (3.4) is highly nonlinear and cannot be solved analytically. However, power counting in the corresponding Martin-Siggia-Rose functional [38] shows that all nonlinear terms in Eq. (3.4) are irrelevant in the renormalization group (RG) sense. This means that the nonlinearities do not change the exponents, but influence only prefactors, etc., in the scaling laws. The linearized form of Eq. (3.4) reads

$$\partial_t h = -\Lambda_0\tilde{\sigma}_0\Delta\Delta h + \nabla\cdot\boldsymbol{\eta}_c \ , \tag{3.5}$$

where $\tilde{\sigma} = \sigma + \sigma''$ is the surface stiffness [39]. The subscript 0 indicates a function evaluated at zero arguments,

e.g., $\Lambda_0 = \Lambda(\nabla h = 0, \kappa = 0)$. The noise correlation function

$$\langle \eta_{c,i}(\mathbf{r},t)\eta_{c,j}(\mathbf{r}',t')\rangle = 2k_BT\Lambda_0\delta_{ij}\delta(\mathbf{r}-\mathbf{r}')\delta(t-t')$$

is given by the fluctuation-dissipation theorem. Setting $D_c = \Lambda_0\tilde{\sigma}_0$, the solution of Eq. (3.5) is given in terms of the Fourier transformed functions by

$$\hat{h}(\mathbf{k},t) = \int_0^t d\tau \, \exp\left[-D_c k^4 (t-\tau)\right] i\mathbf{k}\cdot\hat{\boldsymbol{\eta}}_c(\mathbf{k},\tau)$$

if we start with a flat surface at $t = 0$. The structure factor

$$S(\mathbf{k},t) = \frac{k_BT}{k^2\tilde{\sigma}_0}\left(1 - \exp\left[-2D_c k^4 t\right]\right) \tag{3.6}$$

has the scaling form (2.5) with the exponents $\gamma = 2$ and $z = 4$. Figure 2 shows the steady-state structure factor $S(\mathbf{k}) = S(\mathbf{k}, t \to \infty)$ for the three values $n = 1, 2, 4$ in one dimension. The data are surprisingly well described by the function $S(\mathbf{k}) = A(n)/(1 - \cos k)$, which is obtained if (3.5) is solved on a discrete lattice with a discretized version of the Laplace operator. The parameter n of the Hamiltonian (2.2) does not change the exponents γ and z, but affects only the surface stiffness showing that the parameter n and the nonlinearities of the model are in fact irrelevant.

To incorporate the deposition due to the incoming beam in MBE the flux F and its fluctuations η with $\langle \eta(\mathbf{r},t)\rangle = 0$, $\langle \eta(\mathbf{r},t)\eta(\mathbf{r}',t')\rangle = 2D\delta(\mathbf{r}-\mathbf{r}')\delta(t-t')$ have to be added to Eq. (3.4). The constant F can be eliminated by transforming to the comoving frame of reference $h(\mathbf{r},t) \to h(\mathbf{r},t) + Ft$, and in the following we will set the mean value of h to zero. The conserved noise $\nabla\cdot\boldsymbol{\eta}_c$ can also be neglected since it is irrelevant in the presence of the nonconserved noise η. The resulting equation

$$\partial_t h = \sqrt{g}\,\Gamma_c \frac{\delta \mathcal{F}}{\delta h} + \eta \tag{3.7}$$

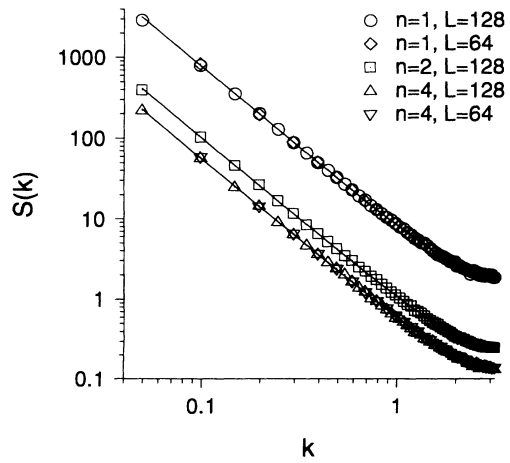

FIG. 2. Equilibrium structure factor ($f = 0$) for $d = 1$ and $k_BT/J = 2$. The solid lines are fits to the form $S(k) = A/(1 - \cos k)$.

is expected to give an accurate description for kinetic roughening of surfaces in MBE in the limit of large length scales and late times where the Langevin description applies. It should be emphasized that the linear version of (3.7) has the same form as (3.5), but with the noise term $\nabla\cdot\boldsymbol{\eta}_c$ replaced by η. In particular, on the right hand side, the leading term involving the height $h(\mathbf{r},t)$ is the fourth derivative $\Delta\Delta h(\mathbf{r},t)$. In this case, however, power counting shows that ∇h has the scaling dimension $(D/D_c)^{1/2}q^{d/2-1}$, where q is an inverse length. All the nonlinear terms in (3.7) with the exception of those due to the curvature dependence of Λ differ from the linear terms by powers of ∇h. Thus these nonlinearities are relevant (marginal) *to all orders* in one (two) dimensions. Therefore, in contrast to the equilibrium case, the linear version of Eq. (3.7) is not a valid approximation for the growth process. Furthermore, a RG calculation for (3.7) is a formidable task and first attempts [40] have only been able to elucidate some aspects of the equation.

If the curvature dependence of Λ is neglected, Eq. (3.7) is invariant under the combined transformation $\mathbf{r} \to -\mathbf{r}$, $h \to -h$. This is a consequence of the assumption that deposition does not change the nature of the diffusion process, i.e., it is still driven by a local free energy functional $\mathcal{F}$. In particular, a so-called conserved KPZ term $\Delta(\nabla h)^2$, which was originally proposed for models with conserved noise [41] but later was also introduced by Villain [18] for models for MBE, does not appear in Eq. (3.7). However, in models with Arrhenius-type hopping rates, the up-down symmetry is lost because of the nature of the dynamics despite the fact that the surface Hamiltonian, which determines the equilibrium properties, does obey this symmetry. In addition, the equilibrium fluctuations are described by (3.5) as we will show in Sec. V. Thus, if the conserved KPZ term appears in the effective Langevin equation, it is entirely due to the nonequilibrium nature of the deposition process. Therefore, it cannot be derived by the arguments leading to Eq. (3.7) since these arguments explicitly separate the effects of the nonconserved noise and the surface dynamics. It is possible that the dynamical coefficient Λ also violates the up-down symmetry, but terms due to this effect appear with higher derivatives than the conserved KPZ term. We include this term in our Langevin equation because it may be required to model the numerical results for driven Arrhenius dynamics without Schwoebel barriers. However, until it is shown that such a term is generated by renormalization of (3.7), its origin remains unclear.

We will show in Sec. IV that a Laplacian term $\nu_2\Delta h$ has to be added to Eq. (3.7) as well [42]:

$$\partial_t h = \nu_2\Delta h + \lambda\Delta(\nabla h)^2 - D_c\Delta\Delta h + \eta\,. \tag{3.8}$$

For $\nu_2 = 0$ this equation [18], in which we have neglected nonlinearities stemming from the surface diffusion, is usually called the conserved KPZ equation. A nonzero ν_2 has its origin in the aforementioned Schwoebel barriers at step edges. It has been shown by Villain [18] that this term appears with a negative coefficient ν_2 for high-symmetry surface orientations. A negative value was

also postulated on different grounds by Golubović and Karunasiri [43], but recent RG calculations [40] for (3.7) disagree with their results. Our results for the $n = 1$ model (see Ref. [10] and Sec. IV) show that an anti-Schwoebel effect with $\nu_2 > 0$ can also occur and this is significant for materials in which atoms jump preferably to the lower terrace at step edges. Replacement and hot atom effects at step edges may also contribute to a positive ν_2 [15]. If $\nu_2 > 0$ all nonlinear terms in (3.7) are irrelevant and we arrive at the Edwards-Wilkinson equation [5]

$$\partial_t h = \nu_2 \Delta h + \eta, \tag{3.9}$$

the solution of which has the same form as (3.6) with $z = 4$ replaced by $z = 2$. The surface roughness diverges only logarithmically ($\zeta = 0$) for $d = 2$ as for a surface in equilibrium above the roughening temperature. Technologically this is the most interesting case since over large length scales the surface is basically flat. For $\nu_2 < 0$ Eq. (3.8) is linearly unstable and consequently the instability has to be controlled by the nonlinear terms. Pyramidal structures seen in experiments [44] are believed to originate from such a Schwoebel effect.

We emphasize that both ν_2 and λ are exactly zero in the equilibrium case (3.6). Therefore, both coefficients are noise generated and have their origin in the nonequilibrium nature of the growth process. Both tend to zero if the noise strength D or, equivalently, the flux F vanishes. There have been attempts to calculate such coefficients from the microscopic properties of growth models by approximating the appropriate master equation by a Fokker-Planck equation [16]. Originally, this approach was used to infer the symmetries of a growth model [45] rather than to calculate coefficients. In fact, such an approach can produce a nonzero ν_2 even for the equilibrium case [45]. Therefore, the results of such a calculation have to be treated with caution as the approximations involved may lead to unphysical terms in the equation of motion. It would be very much preferable to understand the properties of Eq. (3.7) under renormalization.

IV. METROPOLIS DYNAMICS

In this section we present numerical results for the model described in Sec. II for Metropolis hopping rates in the driven case $f > 0$ for two-dimensional substrates. Parts of this work have been published earlier [9,10]. We have carried out simulations for various substrate temperatures and deposition rates f. In no case did we find that these parameters affected the exponents in the asymptotic regime. They do strongly affect the time needed to reach the steady state, as is already clear from the discussion of RHEED oscillations in Sec. II: For small f the oscillations are visible for many deposited layers whereas for large f they do not appear at all and the regime of kinetic roughening is reached earlier. However, we find that the exponents ζ and z *do* depend on the parameter n of the microscopic Hamiltonian (2.2) in contrast to the equilibrium case (see Fig. 2). We therefore discuss the results for different values of n in separate subsections.

A. The $n = 2$ model

We begin our discussion with the $n = 2$ model since it turns out to be a special case and the results for $n \neq 2$ are easier to understand in the light of these results. Figure 3 shows the steady-state structure factor for the two-dimensional $n = 2$ model. $S(k)$ diverges as $k^{-\gamma}$ with $\gamma = 4$ in the limit $k \to 0$. This result is also obtained from the linearized version of Eq. (3.7), which is identical to Eq. (3.8) if ν_2 and λ are set to zero. The structure factor obtained from that linear equation has the same form as (3.6) with $\gamma = 2$ replaced by $\gamma = 4$. As explained in Sec. III, this linear equation is not a valid approximation to Eq. (3.7). That we obtain those results, nevertheless, has its origin in an extra symmetry of the $n = 2$ model [46]. The energy change due to a diffusive move from site i to site j depends only on the third derivative of h: $\Delta\mathcal{H}_{i\to j} = 2J(2d + 1 - \partial_x \Delta h_i)$, where we defined the direction of the move as the positive x direction and the derivatives have to be interpreted in their discrete version, e.g., $\Delta h_i = \sum_{\langle l \rangle_i} (h_l - h_i)$, where $\langle l \rangle_i$ denotes the nearest neighbor sites of i. Therefore, the hopping rates $w_{i\to j}$ are invariant under the transformation

$$h_i \to h_i + \mathbf{x}_i \cdot \mathbf{m} \tag{4.1}$$

if m is an integer. $\mathbf{x}_i$ is the spacial coordinate belonging to site i and $\mathbf{m} = (m, 0)$ or $\mathbf{m} = (0, m)$. Thus the surface growth will evolve in exactly the same way regardless of whether we use periodic boundary conditions or impose a tilt m through the boundary conditions. It has been shown [47] that the coefficient ν_2 can be calculated by measuring the surface current for tilted substrates. Since such a current is zero for periodic boundary conditions by symmetry, (4.1) shows that the current, and therefore ν_2, must be zero for tilted substrates with integer slope

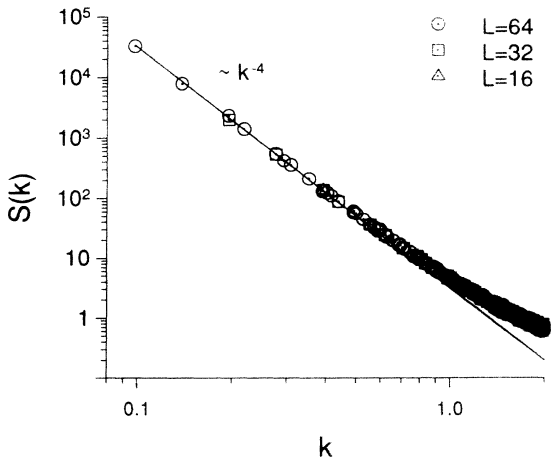

FIG. 3. Steady-state structure factor for the $n = 2$ model ($d = 2$ $k_BT/J = 0.2$, and $f = 0.1$).

m as well. It then follows from a renormalization group argument (see the Appendix) that the height can appear on the right hand side of the Langevin equation describing the $n = 2$ model only in the form $\nabla\Delta h$ or with higher derivatives of h. Since nonlinear functions of these higher derivatives are irrelevant, the linear equation

$$\partial_t h = -D_c \Delta\Delta h + \eta \tag{4.2}$$

is obtained.

This argument is confirmed by the behavior of steady-state autocorrelation function $\Phi(\mathbf{k}, t)$, which collapses to a single curve if plotted as a function of the scaling argument $k^z t$ with $z = 4$ (see Fig. 4). The value of z obeys the hyperscaling relation (2.6). The additional symmetry of the $n = 2$ model, which disallows the Laplacian term and the nonlinearities present in Eq. (3.7), makes this model rather untypical and, in fact, unphysical. It is not surprising that the $n = 2$ model is the only model [48] in the literature that shows the same scaling behavior as the linear equation (4.2). It would be very surprising to find this symmetry in nature.

Figure 5 shows a typical steady-state configuration of the $n = 2$ model. Due to the large roughness exponent $\zeta = 1$ corresponding to the k^{-4} power law of $S(k, t)$ the long-wavelength fluctuations are quite pronounced. We will discuss this type of rough surface further after the discussion of the $n = 1$ and $n = 4$ models.

B. The $n = 1$ model

From a microscopic point of view, the Hamiltonian (2.2) best represents the type of chemical bonding that one expects in a growing film when $n = 1$: the function $|h_i - h_j|$ simply counts the number of dangling lateral bonds in the simple cubic structure and this should be a reasonable approximation to the short range interaction in real systems. As pointed out in Sec. II, the parameter n affects the diffusion of particles in the vicinity of steps and therefore the size and nature of Schwoebel barriers. We show here that in the case $n = 1$ the system in effect has a negative Schwoebel effect and that the appropriate long-wavelength description is the Edwards-Wilkinson equation (3.9). The evidence for this is contained in Figs. 6 and 7 where the steady-state structure factor $S(k)$ and the time-dependent correlation function $\Phi(k, t)$ (2.8) are plotted for several values of L for $T = 0.2J/k_B$ and, in the case of $S(\mathbf{k}, t)$, for another temperature $T = 2J/k_B$ that is above the equilibrium roughening temperature. Obviously, this equilibrium phase transition at $T = T_R \simeq 1.2J/k_B$ [49] does not affect the nonequilibrium steady state of the model. The structure factor shows a clear k^{-2} power law at long wavelengths signaling the presence of the Edwards-Wilkinson term in the Langevin equation. Similarly, the data for $\Phi(k, t)$ falls on a single curve when plotted as function of $k^2 t$ confirming $z = \gamma = 2$.

The existence of the Edwards-Wilkinson term in the Langevin equation for the $n = 1$ model was first inferred

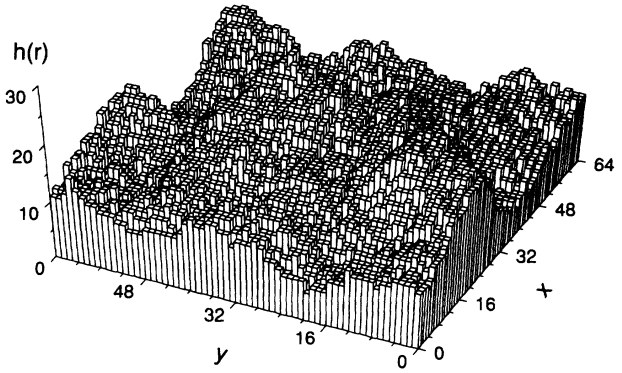

FIG. 5. Steady-state surface configuration of the $n = 2$ model for $L^2 = 64 \times 64$, $k_BT/J = 0.2$, and $f = 0.1$, 4×10^5 monolayers deposited.

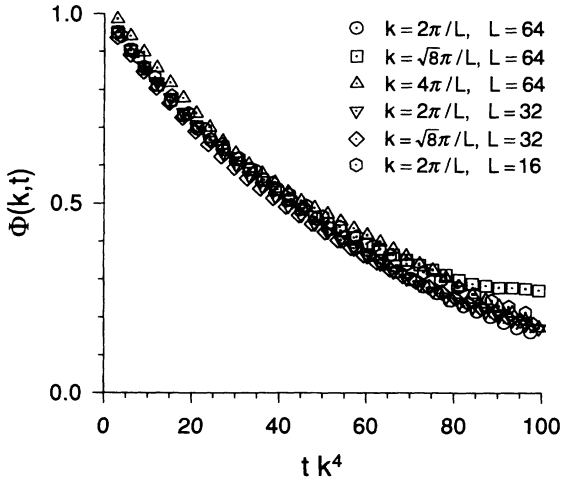

FIG. 4. Steady-state autocorrelation function $\Phi(k, t)$ of Eq. (2.8) for the $n = 2$ model plotted as a function of the scaled variable $k^z t$ with $z = 4$ for several of the smallest values of k for $L = 16$, 32, and 64 ($d = 2$, $k_BT/J = 0.2$, and $f = 0.1$).

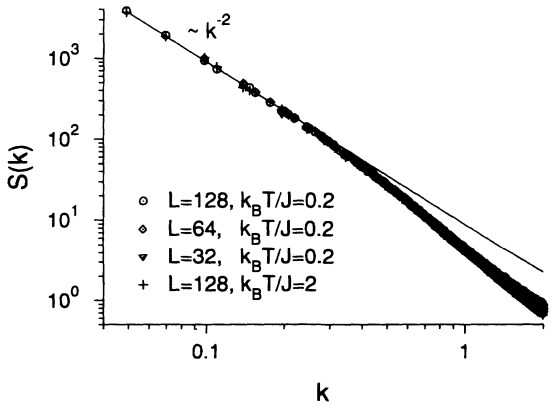

FIG. 6. Steady-state structure factor for the $n = 1$ model at $T = 0.2J/k_B$ and $T = 2J/k_B$ ($d = 2$, and $f = 0.1$).

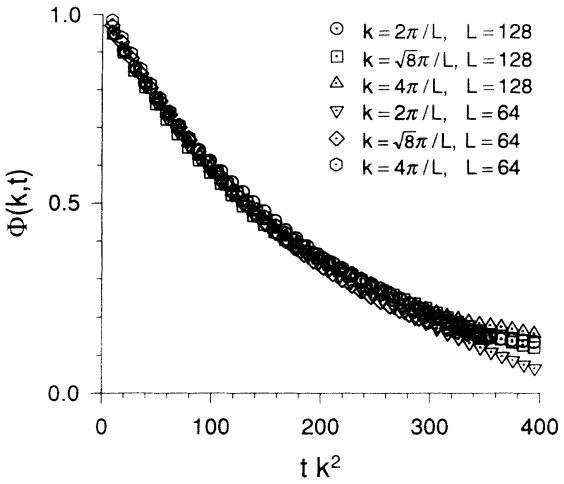

FIG. 7. Steady-state autocorrelation function for the $n = 1$ model plotted as a function of the scaled variable $k^z t$ with $z = 2$ ($d = 2$, $k_B T/J = 0.2$, and $f = 0.1$).

in [10]. In fact, this is the first model for which it was shown that it is possible to have only logarithmic surface roughness in MBE growth modeled by equations of type (1.2). All previous models of the Wolf-Villain type resulted in a much larger surface roughness. Further evidence of the Edwards-Wilkinson behavior was presented, for the one-dimensional case, in [47] where the surface diffusion currents were measured as function of overall tilt of the interface. It was found that $j(m) = -cm$ for small $m = \partial h/\partial x$ and Eq. (1.2) thus ensures the presence of the Laplacian in the Langevin equation. A downhill current corresponds, in the context of anisotropic diffusion near steps, to a negative Schwoebel barrier. In that language, the probability of a particle hopping to a lower terrace from above is larger than the hopping probability on a perfectly flat terrace. We have indicated in Sec. II that in the $n = 1$ model there is no energy cost associated with approaching a step-edge from above (in contrast to the cases $n = 2$,4). However, this is not sufficient to show microscopically that there is such a negative Schwoebel effect. Indeed, we have not been able to prove analytically the existence of a downhill current in the limit of widely separated steps. The effect seems to be a cooperative one: Steps organize themselves into step trains and, in that limit, one can see that there may be a downhill current. Consider a sequence of steps separated by flat sections exactly one site wide and terminating in a flat section at the top and a trough one site wide at the bottom. A particle deposited on this section of the surface executes an unbiased random walk as long as it is not within one step of the upper and lower boundaries. At low temperatures, a hop to the upper terrace is strongly suppressed since an extra two broken bonds are created by such a hop. Conversely, a step into the trough removes two dangling bonds. Thus one can imagine that if a current exists it will be downhill. The configuration discussed here is rather special. We emphasize, however, that we have not been able to construct *any* configuration that would lead to an uphill current for one-dimensional surfaces. A second argument for this conclusion is the following. In the class of models defined by (2.2) we would expect the parameter $j'(m)|_{m=0}$ to vary smoothly with n. We have shown above that for $n = 2$, $j(m) = 0$ for all m. Since increasing n increases the Schwoebel barriers, it is not surprising that $n < 2$ should be characterized by a negative Schwoebel effect [50].

In Fig. 8 we show a typical steady-state configuration of the $n = 1$ model for $T = 0$. The scale of the roughness is comparable to that of the corresponding Fig. 5 of the $n = 2$ model, but the long-wavelength modes are far less prominent. This is not surprising since the structure factor of the $n = 2$ model, because of the k^{-4} divergence at small k, strongly emphasizes the largest wavelengths.

C. The $n = 4$ model

From the discussion in the preceding subsections one expects that models with $n > 2$ are described by a Langevin equation with a negative Laplacian term ($\nu_2 < 0$). In this case the equation of motion for the surface becomes linearly unstable and only the nonlinear effects can stabilize the growth. Microscopically, the Schwoebel barriers at step edges are responsible for such an instability. In this subsection we elucidate these phenomena in the $n = 4$ model [9]. In Fig. 9 we show the steady-state profile of the surface in a system of 64×64 lattice sites. We emphasize the difference in the vertical scale in comparison with Figs. 5 and 8. The nontrivial character of this pyramidal structure becomes apparent when one examines the corresponding structure factor (Fig. 10). $S(\mathbf{k})$ is orders of magnitudes larger for

$$\mathbf{k} = \frac{2\pi}{L}(m_x, m_y), \quad \begin{cases} m_x = 1,3,5,\ldots;\ m_y = 0 \\ m_x = 0;\ m_y = 1,3,5,\ldots \end{cases} \tag{4.3}$$

than for the other modes. Obviously, the structure factor shown in Fig. 10 does not obey the scaling law (2.5). The oscillations in $S(k,t)$ are the signature of the pyramidal surface structure seen in Fig. 9. This kind of pattern formation can be interpreted as a kinetic phase transi-

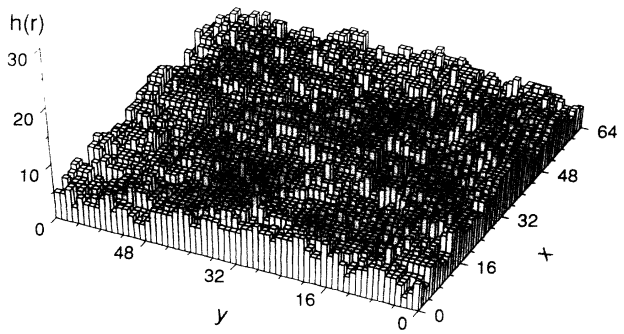

FIG. 8. Typical steady-state configuration for the $n = 1$ model ($L^2 = 64 \times 64$, $k_B T/J = 0.2$, and $f = 0.1$), 10^4 monolayers deposited.

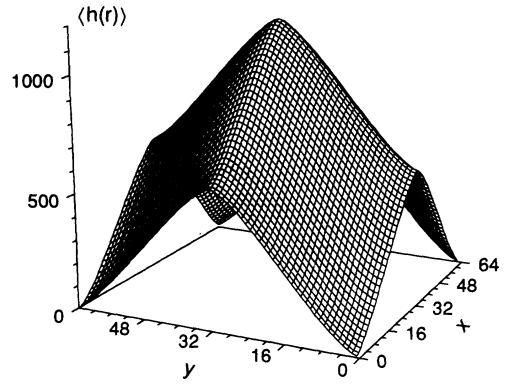

FIG. 9. Pyramidal surface configuration of the $n = 4$ model in the steady state ($L^2 = 64 \times 64$, $k_BT/J = 0.2$, $f = 0.1$, and 4×10^5 monolayers deposited) obtained using the averaging procedure described in the text.

tion from a state with $\langle \hat{h}(\mathbf{k}) \rangle = 0$ to a state with broken translational invariance $\langle \hat{h}(\mathbf{k}) \rangle \neq 0$. This dynamical phase transition exists even in one dimension [9]. We note that the wavelength of the profile is set by the system size L rather than some smaller length. This is a deficiency of the model, which does not include a mechanism that limits the slope of the profile. In fact, the height differences in the steady-state profile, Fig. 9, are so large that the imposed SOS condition is physically meaningless since overhangs would naturally occur before the profile is fully developed. Therefore, the final profile of the $n = 4$ model is not of great physical relevance, but the onset of the instability has its origin in the same kind of Schwoebel barriers, which led to similar pattern formation in some experiments [44].

The breaking of a continuous symmetry such as we have here implies the existence of a Goldstone mode that translates the entire structure on the lattice. Thus, to calculate the average height profile itself, we always moved the minimum of the configuration to the origin before averaging. The profile $\langle \hat{h}(\mathbf{k}) \rangle$ determined in this way is the Fourier transform of the profile shown in Fig. 9 and shows the same oscillations as $S(\mathbf{k})$. In the usual case of surface roughening as in the $n = 1,2$ models the same procedure would yield a completely different result: Shifting the minimum to the origin would single out the smallest $\mathbf{k}$ modes, $\mathbf{k} = 2\pi(1,0)/L$ and $\mathbf{k} = 2\pi(0,1)/L$. Thus the height configuration would be a simple sine-wave profile. The contribution from all other $\mathbf{k}$ modes would be zero, since their phases are random and not related to the phase of the smallest $\mathbf{k}$ mode. In the $n = 4$ model there is *phase coherence* between the $\mathbf{k}$ modes (4.3) so that shifting the minimum to the origin affects all of these modes so that they are not averaged to zero. This phase coherence is probably the clearest characterization of the grooved state of the $n = 4$ model in contrast to the rough surfaces of models without instabilities like the $n = 1,2$ models [51].

Due to the breaking of the translational symmetry $S(\mathbf{k})$ is dominated by the height profile in the $n = 4$ model. To calculate the fluctuations around that profile we define the reduced structure factor as

$$C(\mathbf{k},t) = \langle \hat{h}(\mathbf{k},t)\hat{h}(-\mathbf{k},t) \rangle - |\langle \hat{h}(\mathbf{k},t) \rangle|^2 . \qquad (4.4)$$

This is a very demanding numerical calculation since the fluctuations result from the subtraction of two large quantities [$|\langle h(\mathbf{k},t) \rangle|^2 \gg C(\mathbf{k},t)$] and many independent runs are needed. As seen in Fig. 11, $C(\mathbf{k}, t \to \infty) \equiv C(\mathbf{k})$ does obey a scaling law analogous to (2.5). The exponent γ is roughly equal to 4. The fact that $\gamma \neq 2$ indicates that the ν_2 term in the Langevin equation describing the fluctuations vanishes in the steady state. Note that all nonlinear terms present in Eq. (3.7) are still allowed for $n = 4$ and we therefore do not necessarily have $\gamma = 4$ as in the $n = 2$ model.

Since it is not immediately clear that the fluctuations around the height profile obey the hyperscaling

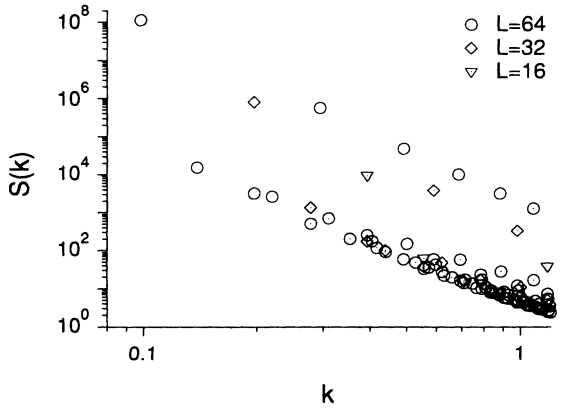

FIG. 10. Violation of the standard scaling assumption (2.5) in the steady-state structure factor of the $n = 4$ model ($d = 2$, $k_BT/J = 0.2$, and $f = 0.1$). The $\mathbf{k}$ modes (4.3) of $S(\mathbf{k})$ for $L = 64$ are given by the Fourier transform of the configuration shown in Fig. 9.

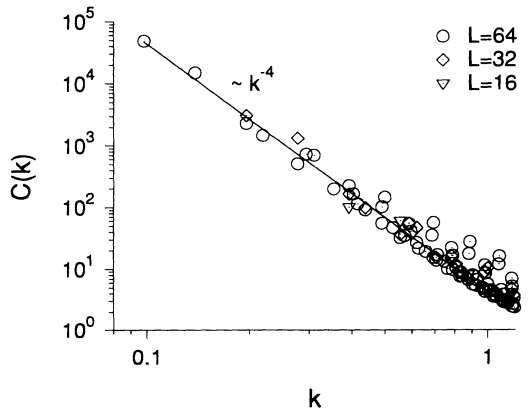

FIG. 11. Reduced steady-state structure factor of the $n = 4$ model obtained after subtracting $|\langle h(\mathbf{k}) \rangle|$ from the structure factor $S(\mathbf{k})$ shown in Fig. 10 ($d = 2$, $k_BT/J = 0.2$, and $f = 0.1$). The solid line corresponds to $C(\mathbf{k}) \sim k^{-4}$.

relation (2.6), one would like to calculate the dynamical exponent z separately in the steady state. This is an even more time-consuming calculation. In the steady state the expectation value $\langle\hat{h}(\mathbf{k},t+t')\hat{h}(-\mathbf{k},t')\rangle \simeq |\langle\hat{h}(\mathbf{k})\rangle|^2 \exp\{-k^2\langle[\Delta\mathbf{x}_0(t)]^2\rangle/2\}$, with $\Delta\mathbf{x}_0(t) = \mathbf{x}_0(t+t') - \mathbf{x}_0(t')$, depends on the drift $\mathbf{x}_0(t)$ of the profile due to the Goldstone mode. Thus, to calculate the appropriate autocorrelation function,

$$\tilde{\Phi}(\mathbf{k},t) = \lim_{t'\to\infty} \frac{1}{C(\mathbf{k},t')}[\langle\hat{h}(\mathbf{k},t+t')\hat{h}(-\mathbf{k},t')\rangle - |\langle\hat{h}(\mathbf{k},t')\rangle|^2 e^{-\frac{k^2}{2}\langle[\Delta\mathbf{x}_0(t)]^2\rangle}], \tag{4.5}$$

$\langle(\Delta\mathbf{x}_0(t))^2\rangle$ has to be determined as well. For $d = 1$ our results show that the profile indeed performs a random walk on the lattice: $\langle(\Delta\mathbf{x}_0(t))^2\rangle \sim t$. The hyperscaling relation (2.6) is fulfilled as well. For $d = 2$ the numerical procedure is so time consuming (about 1000 independent runs are necessary) that we were not able to obtain reliable results.

Figure 12 shows the increase of the surface width of the one-dimensional $n = 4$ model as function of time. In the initial regime T_{I}, we find a surprisingly slow growth with an effective exponent $\zeta/z \simeq 0.25$. Such small initial values close to the Edwards-Wilkinson value of $1/4$ are also typical for KPZ-like models [52,53]. This already shows that it can be misleading to classify models using the scaling behavior of the width, especially if only short times are considered. Before finite size effects become apparent, in regime T_{III}, there is a fairly large regime T_{II} with an effective exponent of roughly 0.61. This value indicates the onset of the instability, since it is larger than $1/2$, the value obtained for random deposition. The regime T_{II} is characterized by a structure factor $S(\mathbf{k},t)$, which has a maximum at a nonzero value of $|\mathbf{k}| = k_{\max}(t)$. It has been argued [43] that the slope ∇h of the surface profile behaves, at least in one dimension, like the order parameter of Ising-like systems in spinodal decomposition. In such ordering processes there exists only one length scale, the domain size $R(t) = 1/k_{\max}(t) \sim t^{1/3}$ [54]. Thus we would conclude that the width should increase like $R(t)$ as well, which disagrees with the result from Fig. 12. The "domain size" can be obtained directly by determining the location of the first zero $r_0(t)$ of the Fourier transform of $S(\mathbf{k},t)$, $g(\mathbf{r},t) = L^{-d}\sum_{\mathbf{r}'}\langle h(\mathbf{r}+\mathbf{r}',t)h(\mathbf{r}',t)\rangle$ [55]. From this one clearly sees (Fig. 13) an increasing wavelength, but the time dependence of $r_0(t)$, displayed in the inset, is characterized by an exponent of 0.17 rather than $1/3$. As pointed out by Krug *et al.* [47] this is a deficiency of the models: To obtain phase separation as in spinodal decomposition the current j as a function of the tilt m has to have a zero at some tilt m_1 that corresponds to another high symmetry surface. The models considered here do not have a high symmetry surface other than $\nabla h = 0$.

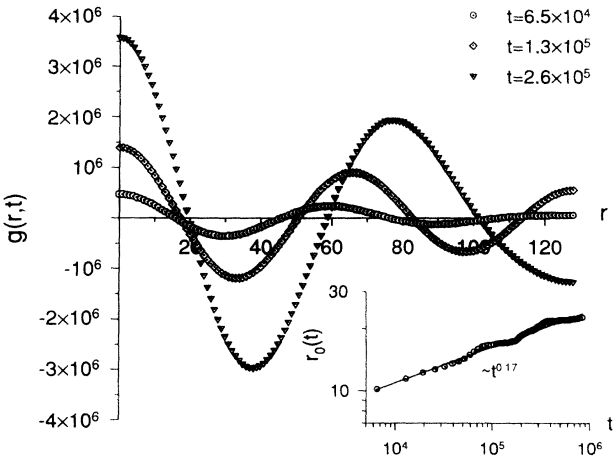

FIG. 13. Real space correlation function $g(r,t)$ as a function of r for several times t. The time dependence of the first zero $r_0(t)$ of $g(r,t)$ is given in the inset ($d = 1$, $L = 256$, $k_BT/J = 100$, and $f = 0.1$).

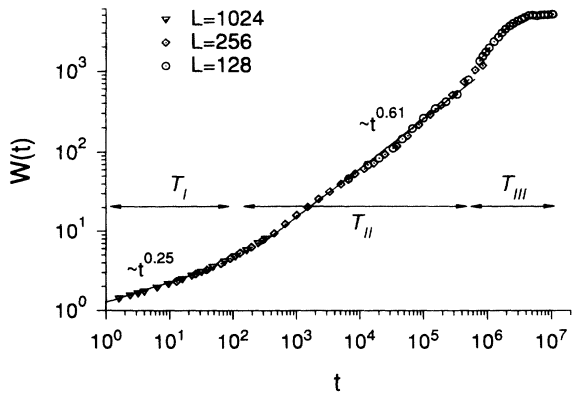

FIG. 12. Time dependence of the surface width in the $n = 4$ model ($d = 1$, $k_BT/J = 100$, and $f = 0.1$). The different regimes T_{I}, T_{II}, and T_{III} are discussed in the text. The time t is measured in numbers of deposited monolayers.

V. ARRHENIUS DYNAMICS

We complete the description of results of our computer simulations by considering the case of Arrhenius dynamics for the $n = 1$ model for $d = 1$. It is generally accepted that surface diffusion is an activated process. In order to hop from one site to another, even if the two sites are equivalent sites on a terrace, a particle must in general cross an energy barrier. These energy barriers are not represented in the SOS Hamiltonians normally used in the description of MBE growth processes. However, it is possible to capture some of the features of activated hopping in the $n = 1$ model [11]. The energy function $\mathcal{H} = \sum_{\langle i,j\rangle}|h_i - h_j|$ is simply the number of unsatisfied lateral bonds. Therefore removing a particle from, e.g., site i increases this number by n_i, where n_i is the number of nearest-neighbor columns of height greater than or equal to h_i. This costs an amount of energy $\epsilon_i = Jn_i$. Thus, if we take

$$w_{i\to j} = \exp\{-\epsilon_i/k_BT\}, \tag{5.1}$$

we have an activated process and have also satisfied detailed balance since

$$\frac{w_{i\to j}}{w_{j\to i}} = \exp\{-(\epsilon_i - \epsilon_j)/k_BT\}.$$

The transition rates (5.1) clearly cannot give rise to the type of slope-dependent current that leads to either the Edwards-Wilkinson scaling or the instabilities discussed in Sec. IV. The probability of a particle hopping from a given site i to *any* of its neighbors is the same—this probability depends only on the coordination number of the hopping particle, not the configuration of the target site. We also note that these transition rates are not invariant under the transformation $h_i \to -h_i$. This has sometimes led to the assumption that the appropriate Langevin equation could contain the conserved KPZ term, even in the case when only equilibrium fluctuations are considered [11].

One can incorporate Schwoebel and anti-Schwoebel effects into these transition rates in a number of ways. Vvedensky *et al.* [15] have discussed this in some detail and have also suggested microscopic mechanisms for an anti-Schwoebel effect. The simplest way to produce a stabilizing downhill current in this context is to modify the transition rates in the vicinity of a step by reducing the energy barrier of a hop from the top of a terrace to the step edge by an amount E_U. This can be done without violating detailed balance [15]. In the simulations discussed below, we have incorporated this effect in one dimension and, for the sake of demonstrating the consequences, have simply taken $E_U = J/2$.

We first discuss the case $f = 0$, i.e., no deposition, with $E_U = 0$. In Fig. 14 we show the steady-state structure factor for $k_BT/J = 1.0$ for one-dimensional systems of size $L \leq 128$. The collapse of the data to a universal curve is excellent and results in an estimate of the exponent $\gamma \approx 1.94$, which is certainly consistent with the value $\gamma = 2$ expected on the basis of Eq. (3.5) and is clearly incompatible with the predictions of the conserved KPZ equation [41], which yields $\gamma = 5/3$. We also show, in Fig. 15, the autocorrelation function $\Phi(k,t)$ (2.8) plotted as function of the scaled variable k^4t. Again, the collapse of the data to a universal curve is quite acceptable, indicating that $z = 4$ as expected. A similar plot with $z = 11/3$ [41] produces much poorer convergence of the data. Therefore, we conclude that although the microscopic dynamics of Eq. (5.1) does not respect the symmetry $h \to -h$ of $\mathcal{H}$, this does not result in symmetry breaking in the Langevin equation.

When the deposition rate f is nonzero, the situation becomes more complicated. In Fig. 16 we show the structure factor in the steady state for $f = 0.05, E_U = 0$, and $k_BT/J = 0.5$. It is clear that, although the values for $S(k)$ for each value of L show reasonably convincing power-law behavior, there is a violation of conventional scaling since the results for different L fall on distinct well-separated curves. Such an effect is also found [8,30] in the Wolf-Villain model [6] and is, in that case, an indicator that large steps in the surface are developing with an L-dependent saturation value of the nearest-neighbor step height. That this occurs also in the case of driven Arrhenius dynamics is demonstrated in Fig. 17, where the function $G(1,t)$ (2.3) is plotted as function of t for several values of L. It is seen that $G(1,t)$ does not saturate for systems as small as $L = 128$ even at $t = 10^6$, where t is measured in *number of layers deposited.* This effect, which seems to be generic in driven models without a stabilizing slope-dependent diffusion current, remains to be explained in a continuum picture. It is certainly difficult to conceive of a single Langevin equation with time-independent coefficients (or, equivalently, L-independent coefficients) that would lead to such behavior. We also

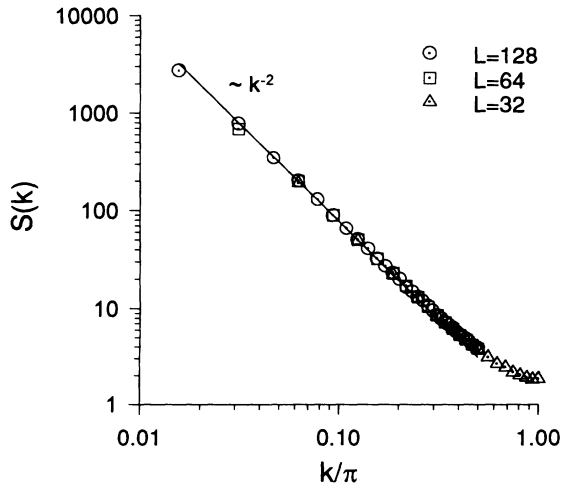

FIG. 14. Steady-state structure factor for the $n = 1$ model with Arrhenius dynamics for $k_BT/J = 1$, $f = 0$, and $d = 1$.

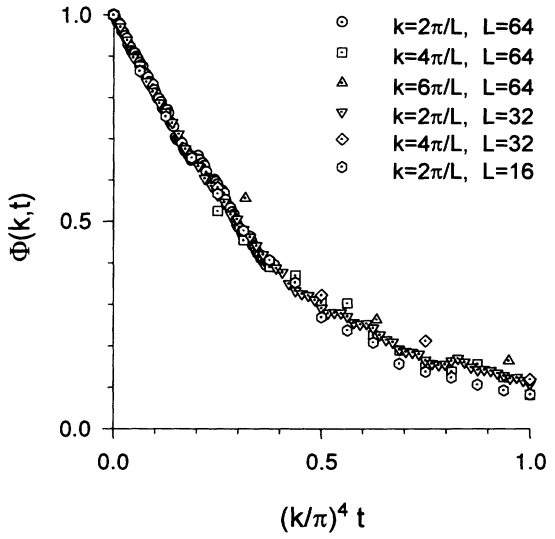

FIG. 15. The function $\Phi(k,t)$ of Eq. (2.8) plotted as a function of the scaled variable k^zt with $z = 4$ for several of the smallest values of k for $L = 16$, 32, and 64 ($d = 1$, $k_BT/J = 1$, and $f = 0$).

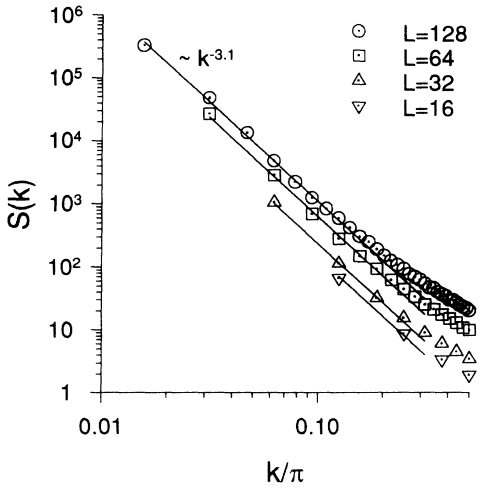

FIG. 16. Steady-state structure factor for $f = 0.05$ and $k_BT/J = 0.5$ for $d = 1$ and various values of L. The straight lines correspond to $S(k) \sim k^{-3.1}$. Note, however, the breakdown of conventional scaling: curves for different L do not fall on a single curve.

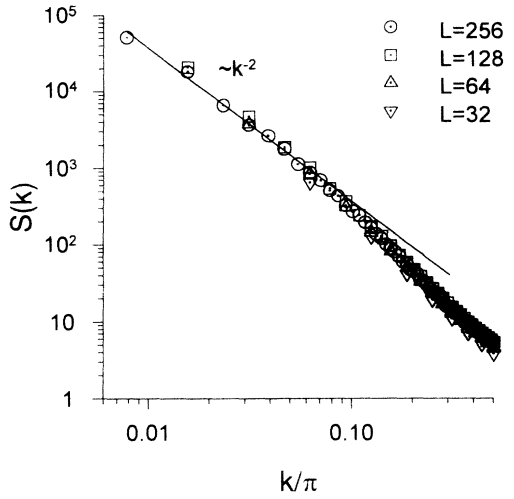

FIG. 18. Steady-state structure factor for Arrhenius diffusion with an "anti-Schwoebel" effect ($d = 1$, $k_BT/J = 0.5$, $E_U = J/2$, and $f = 0.1$). The straight line, drawn as a guide to the eye, corresponds to Edwards-Wilkinson scaling with $\gamma = 2$.

note that the exponent $\gamma \approx 3$ measured from the set of $S(k)$ curves is consistent with the predictions of the conserved KPZ equation [(3.8) with $\nu_2 = 0$], but as pointed out above, this equation cannot explain the breakdown of conventional scaling seen in Fig. 17.

Finally, in Fig. 18 we show the steady-state structure factor for the case of an anti-Schwoebel effect generated (in $d = 1$) in the way discussed above. For systems of size $L \geq 128$ the crossover to Edwards-Wilkinson scaling is essentially complete: The function $S(k) = 3.6(k/\pi)^{-2}$ provides an excellent fit to the structure factor for small k. Conversely, when positive Schwoebel barriers are incorporated into the transition probabilities, e.g., by taking $E_U < 0$, unstable growth of the type seen in the $n = 4$ model discussed above results.

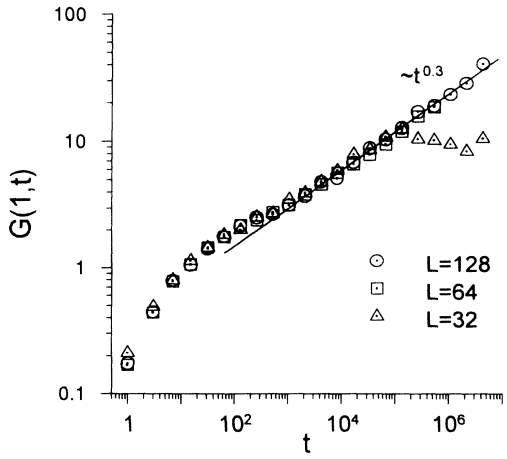

FIG. 17. The function $G(1,t)$ (2.3) for $d = 1$, $f = 0.05$, and $\exp\{-J/k_BT\} = 0.5$. The straight line corresponds to $G(1,t) \sim t^{0.3}$.

VI. CONCLUSION

In this article we have shown that when a realistic surface diffusion mechanism is combined with random deposition there are two generic classes of growth. In the case of positive Schwoebel barriers, growth is unstable and results, in our models, in the formation of large slopes or pyramids. Because these models do not have a second length scale that controls the size of the pyramids, or equivalently limits the slope, they are not directly comparable with real materials. However, we note that unstable growth of the type that occurs in these models has certainly been observed [44]. In the case of such unstable growth, scenarios other than the formation of pyramids are possible, depending on the relevant time scales and length scales. For example, if voids and overhangs form before the three-dimensional structure is fully established, the system may be described by the KPZ equation. To fully explore the phase diagram in this growth regime one must include more realistic surface energies and crystal structures.

The second of the generic cases is perhaps even more interesting than the case of unstable growth. In the context of our models this class is characterized by a negative Schwoebel effect and results in surfaces that are only logarithmically rough. This may be relevant for a large number of experimental systems that typically have much less roughness than previous models [6,7] are capable of predicting. This class of models is described at long length scales by the Edwards-Wilkinson equation, which yields a structure factor that varies as k^{-2} for small k. The structure factor can be measured by light scattering and recent measurements [56] on MBE-grown GaAs have yielded this characteristic k^{-2} behavior.

To make further progress in modeling MBE growth it will be necessary to generalize and augment the models

discussed here. More realistic crystal structures, crystalline anisotropies, and more realistic interactions between particles could have important effects on the length scales and time scales on which the phenomena discussed here will appear.

ACKNOWLEDGMENTS

We thank Joachim Krug, Joel Shore, Tao Sun, Tom Tiedje, Dietrich Wolf, and Andy Zangwill for stimulating conversations and correspondence. This research was supported by the Deutsche Forschungsgemeinschaft within SFB166 and by the NSERC of Canada.

APPENDIX

From the master equation for the $n = 2$ model (see [45,15]) one obtains the equation

$$\partial_t \langle h_i \rangle = \sum_{\langle j \rangle_i} \langle w_{j \to i} - w_{i \to j} \rangle \tag{A1}$$

for the expectation value of the height. It now has been argued [16] that the Langevin equation

$$\partial_t h_i = \sum_{\langle j \rangle_i} (w_{j \to i} - w_{i \to j}) + \eta_i \tag{A2}$$

gives a valid description of the dynamics of the system if the correlations of the noise η_i are determined by the second moment of the master equation. But the variables h_i in Eqs. (A1) and (A2) are in fact different: h_i in (A1) is a *discrete* variable which is defined only for multiples of the lattice constant, whereas h_i in (A2) is a *continuous* variable. Therefore, a derivation of the continuum limit leading from (A1) to (A2) is required. This is highly nontrivial and no general procedures are available.

As mentioned in the text, the hopping rates $w_{i \to j}$ of the $n = 2$ model are especially simple; they depend only on $\partial_x \Delta h_i$. This extra symmetry allows us to illustrate why the coefficient ν_2 in the Langevin equation for the $n = 2$ model is zero. To obtain the continuum limit a coarse graining procedure has to be carried out. For the sake of clarity we restrict ourselves to $d = 1$. Derivatives are defined in the following way:

$$\partial_x^n h_i \equiv \begin{cases} \partial_x^{n-1} h_i - \partial_x^{n-1} h_{i-1} , & n \text{ odd} \\ \partial_x^{n-1} h_{i+1} - \partial_x^{n-1} h_i , & n \text{ even} \end{cases} \qquad \partial_x^0 h_i \equiv h_i .$$

Furthermore, we define the coarse grained variables as

$$h_i^{(r)} = \tfrac{1}{4}(h_{i+1}^{(r-1)} + 2h_i^{(r-1)} + h_{i-1}^{(r-1)}) \tag{A3}$$

with $h_i^{(0)} \equiv h_i$. The iteration of (A3) leads to a successive elimination of the short wavelengths, e.g., $\hat{h}^{(1)}(k = \pi) = 0$, as it should be in such a real space renormalization procedure. As a consequence, Eq. (A3) cannot be inverted, but we can eliminate the old variables using the identity

$$\partial_x^n h_i^{(1)} = \partial_x^n h_i + \tfrac{1}{4} \partial_x^{n+2} h_i ,$$

which leads to

$$\partial_x^n h_i = \partial_x^n h_i^{(1)} + \sum_{l=1}^{\infty} \left(-\tfrac{1}{4}\right)^l \partial_x^{n+2l} h_i^{(1)} . \tag{A4}$$

The lowest derivative, which appears on the right hand side of Eq. (A1), is $\partial_x^3 h$. The coarse graining procedure (A3) does not introduce lower derivatives. Thus it is conceivable that the coefficient ν_2 in the Langevin equation for the continuous height variable $\bar{h}_i \equiv \lim_{r \to \infty} h_i^{(r)}$ is indeed zero. The argument relies crucially on the fact that the higher order derivatives that are generated in the coarse graining procedure are irrelevant and that the lowest derivatives appearing in the hopping rates $w_{i \to j}$ are of third order. Thus the same argument fails for the $n = 1$ and $n = 4$ models.

[1] M. Eden, in *Symposium on Information Theory in Biology*, edited by H. P. Yockey (Pergamon, New York, 1958), p. 359.
[2] M. J. Vold, J. Colloid Sci. **14**, 168 (1959).
[3] M. Plischke, Z. Rácz, and D. Liu, Phys. Rev. B **35**, 3485 (1987); J. M. Kim and J. M. Kosterlitz, Phys. Rev. Lett. **62**, 2289 (1989); P. Meakin, P. Ramanlal, L. Sander, and R. C. Ball, Phys. Rev. A **34**, 5091 (1986).
[4] M. Kardar, G. Parisi, and Y.-C. Zhang, Phys. Rev. Lett. **56**, 889 (1986).
[5] S. F. Edwards and D. R. Wilkinson, Proc. R. Soc. London Ser. A **381**, 17 (1982).
[6] D. E. Wolf and J. Villain, Europhys. Lett. **13**, 389 (1990).
[7] S. Das Sarma and P. Tamborenea, Phys. Rev. Lett. **66**, 325 (1991).
[8] M. Schroeder, M. Siegert, D. E. Wolf, J. D. Shore, and M. Plischke, Europhys. Lett. **24**, 563 (1993).
[9] M. Siegert and M. Plischke, Phys. Rev. Lett. **68**, 2035 (1992).
[10] M. Siegert and M. Plischke, J. Phys. I **3**, 1371 (1993).
[11] M. R. Wilby, D. D. Vvedensky, and A. Zangwill, Phys. Rev. B **46**, 12896 (1992); **47**, 16068 (1993).
[12] D. A. Kessler and B. G. Orr (unpublished).
[13] We use the term "Metropolis dynamics" to denote any transition rate that depends on the energy difference between the initial and final states. In fact, the transition rates (2.1) are those of R. J. Glauber, J. Math. Phys. **4**, 294 (1963), rather than the Metropolis transition rates commonly used in equilibrium Monte Carlo simulations.
[14] R. L. Schwoebel and E. J. Shipsey, J. Appl. Phys. **37**, 3682 (1966); R. L. Schwoebel, *ibid.* **40**, 614 (1969); G. Ehrlich and F.G. Hudda, J. Chem. Phys. **44**, 1039 (1966); S. C. Wang and G. Ehrlich, Phys. Rev. Lett. **70**, 41 (1993).

[15] D. D. Vvedensky, A. Zangwill, C. N. Luse, and M. R. Wilby, Phys. Rev. E **48**, 852 (1993).

[16] A. Zangwill, C. N. Luse, D. D. Vvedensky, and M. R. Wilby, Surf. Sci. **274**, L529 (1992); in *Interface Dynamics and Growth*, edited by K. S. Liang, M. P. Andersson, R. F. Bruinsma, and G. Scoles, MRS Symposia Proceedings No. 237 (Materials Research Society, Pittsburgh, 1992), pp. 189–198.

[17] P. Šmilauer, M. R. Wilby, and D. D. Vvedensky, Phys. Rev. B **47**, 4119 (1993); **48**, 4968 (1993); Surf. Sci. **291**, L733 (1993); M. D. Johnson, C. Orme, A. W. Hunt, D. Graff, J. Sudijono, L. M. Sander, and B. G. Orr, Phys. Rev. Lett. **72**, 116 (1994).

[18] J. Villain, J. Phys. I **1**, 19 (1991).

[19] J. Villain, A. Pimpinelli, L.-H. Tang, and D. E. Wolf, J. Phys. I (Paris) **2**, 2107 (1992); J. Villain, A. Pimpinelli, and D. E. Wolf, Comments Condens. Matter Phys. **16**, 1 (1992).

[20] S. Stoyanov and D. Kashchiev, in *Current Topics in Materials Science*, edited by E. Kaldis (North-Holland, Amsterdam, 1981), Vol. 7.

[21] Y. W. Mo, J. Kleiner, M. B. Webb, and M. G. Lagally, Phys. Rev. Lett. **66**, 1998 (1991); E. Kopatzki, S. Günther, W. Nichtl-Pecher, and R. J. Brehm, *ibid.* **284**, 154 (1993).

[22] J. Sudijono, M. D. Johnson, M. B. Elowitz, C. W. Snyder, and B. G. Orr, Surf. Sci. **280**, 247 (1993).

[23] D. D. Vvedensky, S. Clarke, K. J. Hugill, A. K. Myers-Beaghton, and M. R. Wilby, in *Kinetics of Ordering and Growth at Surfaces*, edited by M. G. Lagally (Plenum, New York, 1990), pp. 297–311.

[24] F. Family and T. Vicsek, J. Phys. A **18**, L75 (1985).

[25] Here and throughout this article, all lengths are measured in units of the lattice constant. The wave vector $\mathbf{k}$ is measured in units of the inverse lattice constant and is reduced to the first Brillouin zone. Times are measured in numbers of deposited monolayers.

[26] M. Plischke and Z. Rácz, Phys. Rev. A **32**, 3825 (1985).

[27] J. L. Goldberg, X.-S. Wang, N. C. Bartelt, and E. D. Williams, Surf. Sci. **249**, L285 (1991); J. Sudijono, M. D. Johnson, C. W. Snyder, M. B. Elowitz, and B. G. Orr, Phys. Rev. Lett. **69**, 2811 (1992); D. E. Savage, E. J. Heller, Y.-H. Phang, M. Schacht, and M. G. Lagally, in *Surface Disordering: Growth, Roughening, and Phase Transitions*, edited by R. Jullien, J. Kertész, P. Meakin, and D. E. Wolf (Nova Science, Commack, NY, 1992); F. Wu, S. G. Jaloviar, D. E. Savage, and M. G. Lagally, Phys. Rev. Lett. **71**, 4190 (1993).

[28] J. G. Amar, P.-M. Lam, and F. Family, Phys. Rev. E **47**, 3242 (1993).

[29] H. Leschhorn and L.-H. Tang, Phys. Rev. Lett. **70**, 2973 (1993).

[30] M. Plischke, J. D. Shore, M. Schroeder, M. Siegert, and D. E. Wolf, Phys. Rev. Lett. **71**, 2509 (1993).

[31] S. Das Sarma and S.V. Ghaisas, Phys. Rev. Lett. **69**, 3762 (1992).

[32] H.-N. Yang, T.-M. Lu, and G.-C. Wang, Phys. Rev. B **47**, 3911 (1993); Phys. Rev. Lett. **68**, 2612 (1992).

[33] J. Villain, D. R. Grempel, and J. Lapujoulade, J. Phys. F **15**, 809 (1985); D. E. Savage, J. Kleiner, N. Schimke, Y.-H. Phang, T. Jankowski, J. Jacobs, R. Kariotis, and M. G. Lagally, J. Appl. Phys. **69**, 1411 (1991); S. K. Sinha, E. B. Sirota, S. Garoff, and H. B. Stanley, Phys. Rev. B **38**, 2297 (1988).

[34] W. W. Mullins, J. Appl. Phys. **28**, 333 (1957); *Metal Surfaces: Structure, Energetics and Kinetics* (American Society for Metals, Metals Park, OH, 1963), p. 17.

[35] C. Herring, in *The Physics of Powder Metallurgy*, edited by W. E. Kingston (McGraw-Hill, New York, 1951), pp. 143–179.

[36] S. T. Chui, J. D. Weeks, Phys. Rev. Lett. **40**, 733 (1978); P. Nozières and F. Gallet, J. Phys. (Paris) **48**, 353 (1987); P. Nozières, in *Solids far from Equilibrium*, edited by C. Godrèche (Cambridge University Press, Cambridge, 1991).

[37] See, e.g., F. David, in *Statistical Mechanics of Membranes and Surfaces*, edited by D. Nelson, T. Piran, and S. Weinberg (World Scientific, Singapore, 1989), p. 157.

[38] P. C. Martin, E. D. Siggia, and H. A. Rose, Phys. Rev. A **8**, 423 (1973); R. Bausch, H. K. Janssen, and H. Wagner, Z. Phys. B **24**, 113 (1976).

[39] The surface tension is a function of the surface normal $\hat{\mathbf{n}} = (-\nabla h, 1)/\sqrt{g}$, which can be parametrized by the two angles ϑ and φ. Here we neglected the (usually small) dependence on the polar angle φ. The prime denotes the derivative with respect to ϑ, which describes the deviation of the surface inclination from the high symmetry surface. For a detailed discussion see P. Nozières, in *Solids far from Equilibrium* (Ref. [36]).

[40] T. Sun and M. Plischke, Phys. Rev. Lett. **71**, 3174 (1993).

[41] T. Sun, H. Guo, and M. Grant, Phys. Rev. A **40**, 6763 (1989).

[42] In principle, also higher order nonlinear terms of the form $\nabla \cdot [\nabla h f((\nabla h)^2)]$ with $f(0) = \nu_2$ have to be included. If $\nu_2 > 0$ these nonlinearities are irrelevant. They are important for the pattern formation in the linearly unstable case of $\nu_2 < 0$.

[43] L. Golubović and R. P. U. Karunasiri, Phys. Rev. Lett. **66**, 3156 (1991).

[44] M. Bott, T. Michely, and G. Comsa, Surf. Sci. **272**, 161 (1992).

[45] Z. Rácz, M. Siegert, D. Liu, and M. Plischke, Phys. Rev. A **43**, 5275 (1991).

[46] We are indebted to Joel Shore for bringing this symmetry to our attention.

[47] J. Krug, M. Plischke, and M. Siegert, Phys. Rev. Lett. **70**, 3271 (1993).

[48] The linear equation (4.2) has been used a number of times to model discrete growth processes, in particular those of the Wolf-Villain type. Recent results [8,30] show convincingly that this is incorrect.

[49] See, e.g., J. D. Weeks and G. H. Gilmer, Adv. Chem. Phys. **40**, 157 (1979).

[50] For $d = 1$, the coefficient $c = j'(m)|_{m=0}$ changes sign precisely at $n = 2$ [Joel Shore (private communication)].

[51] In contrast to previous statements [28], the sine-wave profiles that are characteristic of rough surfaces are always obtained, independently of the size of the roughness exponent ζ, when averaging over the shifted configurations as long as $S(\mathbf{k})$ diverges for $k \to 0$. The shift procedure simply singles out the smallest $\mathbf{k}$-mode and, if averaged over a sufficient number of runs, such a profile would even be obtained in the $n = 1$ model.

[52] J. G. Zabolitzky and D. Stauffer, Phys. Rev. A **34**, 1523 (1986).

[53] D. A. Kessler, H. Levine, and L. M. Sander, Phys. Rev. Lett. **69**, 100 (1992).

[54] For an overview see J. S. Langer, in *Solids far from Equi-*

librium, edited by C. Godrèche (Cambridge University Press, Cambridge, 1991); see also, A. J. Bray, Phys. Rev. Lett. **62**, 2841 (1989); Phys. Rev. B **41**, 6724 (1990). The somewhat artificial case of spinodal decomposition in $d = 1$ has been discussed by T. Kawakatsu and T. Munakata, Prog. Theor. Phys. **74**, 11 (1985).

[55] T. M. Rogers, K. R. Elder, and R. C. Desai, Phys. Rev. B **37**, 9638 (1988).

[56] C. Lavoie, M. Nissen, and T. Tiedje (unpublished).

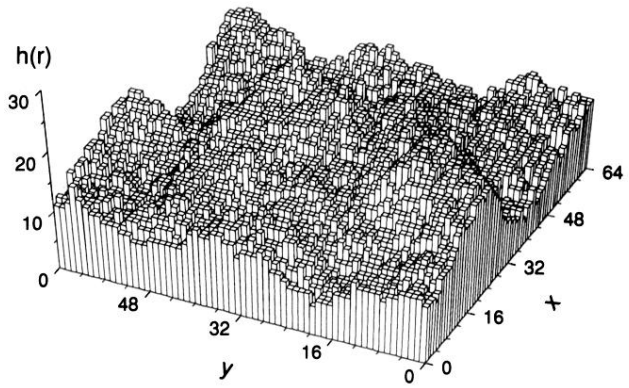

FIG. 5. Steady-state surface configuration of the $n = 2$ model for $L^2 = 64 \times 64$, $k_B T/J = 0.2$, and $f = 0.1$, 4×10^5 monolayers deposited.

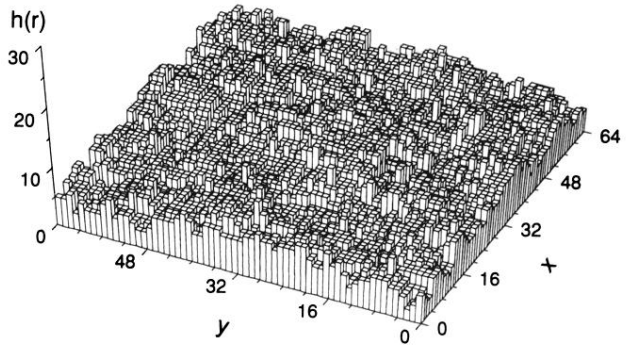

FIG. 8. Typical steady-state configuration for the $n = 1$ model ($L^2 = 64 \times 64$, $k_B T/J = 0.2$, and $f = 0.1$), 10^4 monolayers deposited.

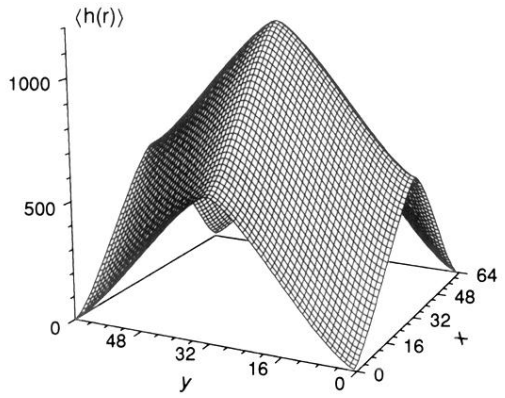

FIG. 9. Pyramidal surface configuration of the $n = 4$ model in the steady state ($L^2 = 64 \times 64$, $k_B T/J = 0.2$, $f = 0.1$, and 4×10^5 monolayers deposited) obtained using the averaging procedure described in the text.